A Spectral Analysis of the Chemical Enrichment History of Red Giants in the Andromeda

Galaxy Field (M31) Versus its Dwarf Spheroidal (dSph) Satellites

By Namrata Anand

The Harker School

I. Introduction

Galaxies are interesting organisms: they move, change, grow, and, strangely enough, consume. In a process known as galaxy cannibalism, an astronomical body, very often a dwarf satellite galaxy, is drawn towards a larger, more massive galaxy, thrust into the process by the forces of gravity (Cox & Loeb 2007). After the meal, what determines whether a dwarf satellite of a galaxy is a separate entity? When does a star become fully incorporated into a galaxy? What are the chemical differences between "primaries" and their satellites?

This project relies on the analysis of the chemical essence of stars to distinguish between Andromeda's (M31) Field stars and the stars of its Dwarf Spheroidal Satellite Galaxies (dSphs). The data used was collected over a period of several years; every star's individual spectrum was obtained through remote observation sessions using major telescopes around the globe. Due to this long process, this study does not involve direct data collection, but rather is a data manipulation and analysis project. Other research conducted alongside this study included finding out how to best extract information from the spectra of M31's Red Giants (RG) (useful for later steps in this analysis) and how to quantify the mix of stellar populations in M31 (Gilbert et. al 2007, Gilbert et. al 2009). Handling the large database of spectral data required Interactive Data Language (IDL) programming in addition to individual analysis. By using specific, detailed criteria to differentiate between the two samples (Field vs. dSph) and by subsequently analyzing the chemical spectra of the two populations both qualitatively and quantitatively, this analysis has exposed key information about the chemical enrichment history of M31.

Astronomical chemical analysis projects have been conducted in the past; in fact, examination of the dSph Satellites around the Milky Way (MW) Galaxy has been promising (Kirby et. al 2009). However, very little has been done to examine the chemical differences

between the MW's sister galaxy, Andromeda, and its dSph Satellites. The signal-to-noise ratios are low in M31, hindering accurate spectroscopy; however, this problem was eliminated by relying on *coadded* rather than individual spectra. Due to the similarities that the MW and M31 share (being relatively close spiral galaxies), this project's findings are somewhat applicable to the MW as well (Yin et. al 2007). Finally, chemical analysis projects, especially ones that focus on patterns of metallicity, have the scope to identify locations with a high probability of extraterrestrial life. The sun, an extremely metal-rich star, is surrounded by equally rich planetary bodies; if pockets of high metallicity are located within Andromeda, scientists can pinpoint these as locations where planetary bodies might be similar to Earth, planets that might have the rich chemical makeup necessary for life (Forgan 2008). Although this conclusion is a large step to take from this study alone, astronomers and astrophysicists can use such chemical abundances projects to build upon their own research, research that can lead to such "astronomical" breakthroughs in the future.

II. Methods

Criteria, both general and specific, were determined to differentiate the analysis sample from a large data set. In order to analyze the chemical differences between M31's Field and dSph stars, it was also imperative to properly distinguish the Field Sample from the Dwarf Sample.

A. Overall Sample Criteria

First, a set of general criteria was used to ensure that all of the stars chosen for analysis were Red Giants (RGs) with relatively clean and accurate spectra.

1. **Zquality equal to 3 or 4**: An IDL-based program called ZSPEC visually examined each spectrum to determine the quality of the data, and assigned 'Zquality' values for each star. Zqualities of -1 were assigned to alignment stars, stars in the Milky Way (MW) Galaxy used

to properly position telescopes, design masks, and to collect data from distant galaxies. Zqualities of 0 were assigned to galaxies and quasi-stellar objects. Zqualities of 1 and 2 were assigned to stars with poor spectra: either the velocities had to be measured manually or could not be derived from the spectra. Finally, Zqualities of 3 or 4 were assigned to stars with marginal velocities gained from cross correlation (3) or for secure velocities gained from cross correlation (4). For example, if a spectrum has a Ca triplet that matches up with a synthetic (model) spectrum, it might be assigned a Zquality value of 3; if it has a Ca triplet, Na doublet, and TiO bands that all match up, the spectrum might be assigned a value of 4. This cut separated stars in Andromeda from alignment stars in the MW as well as from other galaxies. Furthermore, this diagnostic ensured that the stars had spectra that could be easily *coadded* (see *Page 8*), from which a clear velocity could be derived, and from which some sort of chemical analysis could be drawn. (conversation with P. Guhathakurta, 2009)

2. **M31Class equal to 1, 2, or 3:** The tag M31Class is pre-assigned to stars when their spectra are collected. Stars' locations, spectra, and telescopic images are analyzed, and then stars are assigned an M31Class value, a ratio of the probability of a star being either a Red Giant (RG) or a foreground dwarf star (Gilbert et. al 2006). Negative values indicate a greater probability of an object being a dwarf star. A value of zero is inconclusive: the object could be either a RG or a dwarf star. Finally, positive values (1, 2, or 3) indicate that the object is more likely a RG. Although most of the stars in M31 are RGs (Côté et. al 2009), this diagnostic is yet another way to differentiate between M31 RGs and *MW* dwarf stars.

B. Dwarf Criteria

The Dwarf Galaxies analyzed in this study were Dwarf Spheroidal Galaxy Satellites (dSphs). Dwarf Irregular (dIrr) Satellites are seen only on the remote outskirts of Andromeda and

there is significant debate over whether they orbit the entire Local Group or simply M31, although significant research has still been conducted with dIrrs (Lee et. al 2003). As there were limited processed spectra from M31's Dwarf Elliptical (dE) Satellites, both dIrrs and dEs have been excluded from the study. Still, dSphs are the most ideal satellite galaxies to observe: they have simple structures (Walker et. al 2007) and have most likely undergone transformations (Smecker-Hane & McWilliam 1999). Although dSphs are usually low-luminosity (Kalirai et. al 2009), three high-luminosity (d1, d2, and d7) and five low-luminosity (d3, d5, d10, d13, and A170 [d14]) dSph satellites were studied. One basic diagnostic was used to differentiate between the RG stars of M31's dSph Satellites and the overall data set:

1. **Stringent Velocity Cuts**: For each dSph, a histogram of Corrected Velocities (Vcorr) with a bin size of 5 was generated. Stars whose corrected velocities lay within the main histogram peak were selected, as these members are stars that are all moving at similar velocities and most likely members of the same dSph population in question. Histograms like *Figure 1* (See *Page 5*) were key in separating dSph stars from Field stars and necessary stars from irrelevant stars. The highest and most negative peaks' stars were separated as members of specific Dwarf Spheroidal Galaxy populations, while the smaller peaks' stars were placed in the M31 Field Population. In rare cases where there were two major peaks within the histogram, as seen in *Figure 1*, only the more negative peaks were selected in order to eliminate the inclusion of stars in the MW Galaxy, stars moving at a distinctly different velocity (Guhathakurta et. al 2009).
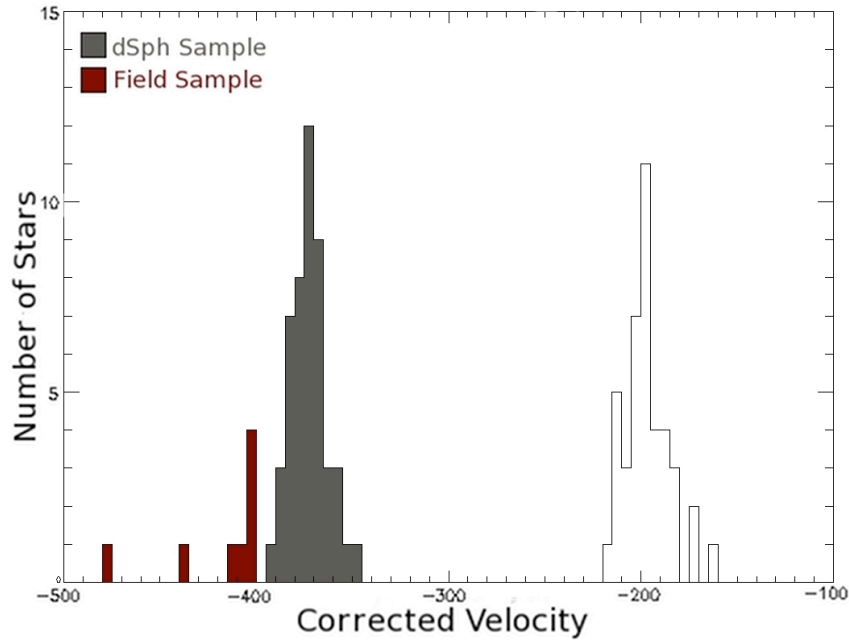
Figure 1: **Example Histogram of Corrected Velocities [kiloparsecs] for Stars in dSph d1 (bin size=5)**

C. Field Criteria

In order to generate the most accurate and, at the same time, the largest Field Sample, certain additional criteria were used to separate the Field Stars from both the dSph Sample and from the overall set of data.

1. **Opposing Velocity Cuts**: Stars from the initial dSph Sample that were not within the stringent Vcorr range selected by dSph Criteria 1 (*Section II.B.1.)* and were also not within a possible MW Galaxy peak were selected as part of the Field Sample (See *Figure 1*).

2. **M31Class 2 or 3**: Red Giants (RGs) cannot be isolated through stringent velocity cuts for stars in M31's Field; they are not moving at a distinctly different velocity from the rest of the galaxy as they are in the case of the dSph Satellites' stars. By requiring a value of 2 or 3 for the field stars' M31Class values, the probability of every star in the sample being an RG is increased further.

All other M31 mask data within the database that followed the criteria stipulated above were placed in the Field Sample set. This additional data consisted of information from nineteen other masks, which included groups of stars at varying radii distances ([kiloparsecs]) from M31's center.

D. Metallicity Graphing

Once the two samples were accurately separated and distinguishable, comparisons of the two could begin. For each sample, Metallicity (FeHphot) vs. Color ($(V-I)_0$) graphs were generated.

1. **FeHphot:** FeHphot or [Fe/H] stands for the ratio of iron to hydrogen in a star. It is a logarithmic unit [dex] and is based around the Sun's [Fe/H] value, which is set at 0 (an FeHphot value of -1, for example, describes a star 10 times more anemic than the sun) (conversation with Guhathakurta, 2009). The calculation of FeHphot (photometrically) is an approximation based on educated assumptions. Stars in a select group are assumed to have the same age, be the same distance away, and have the same ratio of alpha elements (Ca, Mg, Al, Ti) to Fe (referred to as $[\alpha/Fe]$). Then, the stars are plotted on a CMD (Color Magnitude Diagram), and, according to the track formed in color magnitude space, are assigned an FeHphot value. This process is effective because a star's position on a CMD is not strongly affected by age or $[\alpha/Fe]$; rather, Metallicity is the important factor (Morossi et. al 2007). Even if the assumptions are wrong, FeHphot is usually correct up to 0.2 [dex]. A star's [Fe/H] can be determined through spectroscopic means as well, and this method can be used as a tool to cross-check the photometric approximation. In M31, most stars have an FeHphot value between -3 and -1; this makes sense, as the sun is extremely enriched, especially in comparison to most stars in Andromeda. (conversation with P. Guhathakurta, 2009)
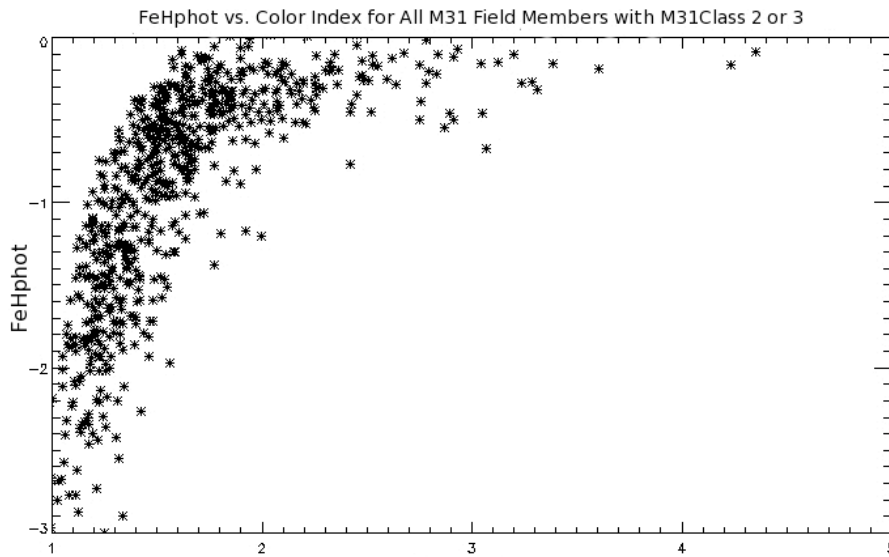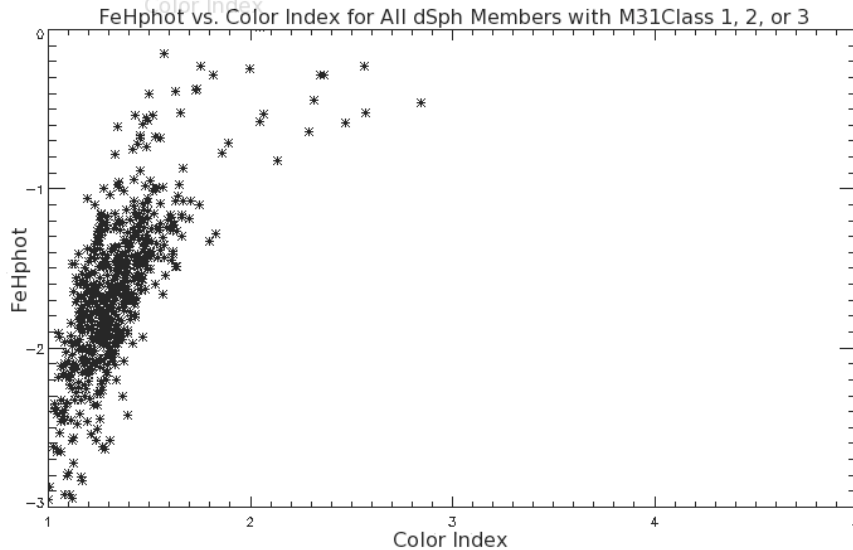
Figure 2:

Metallicity Graph ([Fe/H] [dex] vs. Vi0 [mag]) for Stars in M31's Field

Figure 3:

Metallicity Graph ([Fe/H] [dex] vs. Vi0 [mag]) for Stars in M31's dSph Satellite Population

E. Binning and Coadding Spectra

The data from each star is not individually relevant or accurate; countless errors can occur when collecting data from hundreds of millions of light years away (Kirby et. al 2009). In addition, comparisons between the Field Sample and the dSph Sample are best done in large groups. Thus, equal-sized bins (0.2 mag x 0.5 dex) were used to grid the Metallicity graphs, and an IDL program was used to coadd the spectra from the stars in each bin. This program first assigned each spectra an ivar value ("inverse of the variance") and then weighted the spectra in

each bin according to the assigned value. Spectra with low 'ivars' (more jagged) were given less weight in the coadding process, while clearer spectra with higher 'ivars' were given more weight. As a result, this program not only coadded data to make chemical trends clearer, but also reduced the effect of systematic data collection errors (bad pixilation and data reduction failures). Still, some bins in remote locations of the metallicity graphs had less than 10 star spectra, compromising the accuracy of the coadded spectra (if a single spectrum in a small bin is a catastrophic failure, it can shift the entire coadded spectrum erroneously). This process was corrected through "adjustable binning." The results of the coaddition process can be seen in *Figures 4* and *5* (below, page 9).

Adjustable Binning *Requirements* (Operational Definition for this study)

- Every bin without at least 10 spectra must be combined with adjacent bins.

- Bins must only be extended in one direction to best preserve the integrity of the data. In this case, the bins were extended horizontally, maintaining the same FeHphot range of 0.5 [dex] while changing in $(V-I)_0$ [mag] ranges.
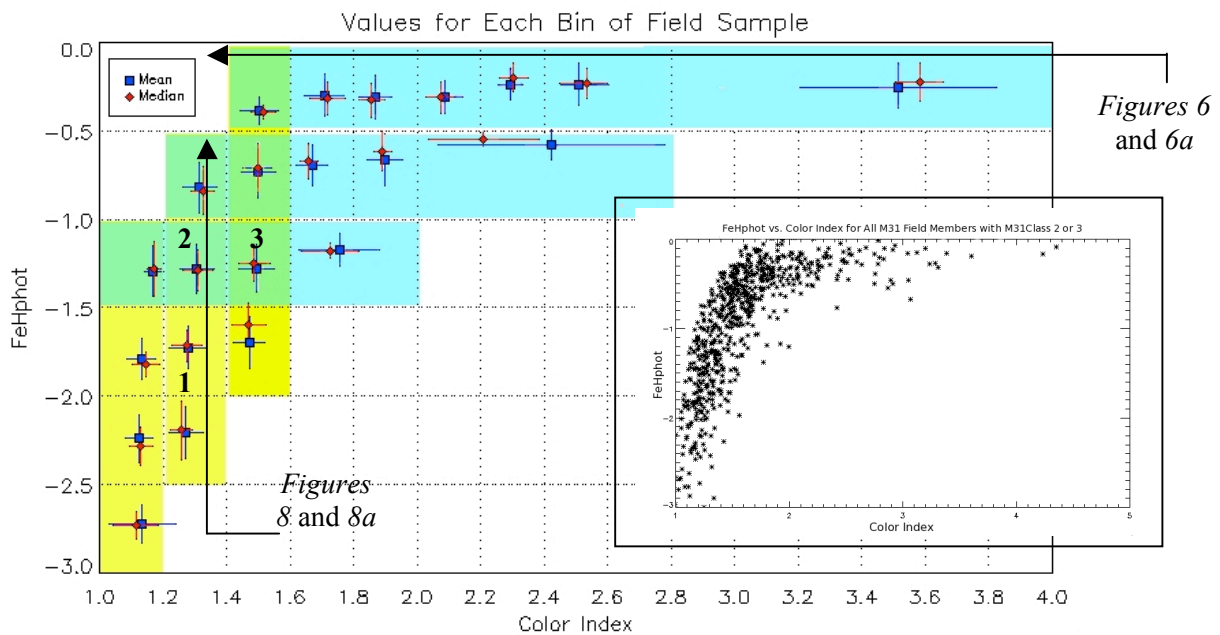

Figure 4: **The Mean and Median Values (with Root Mean Square Deviation) of Metallicity vs. Color for the Coadded Spectra of Each Bin of the M31 Field Sample**
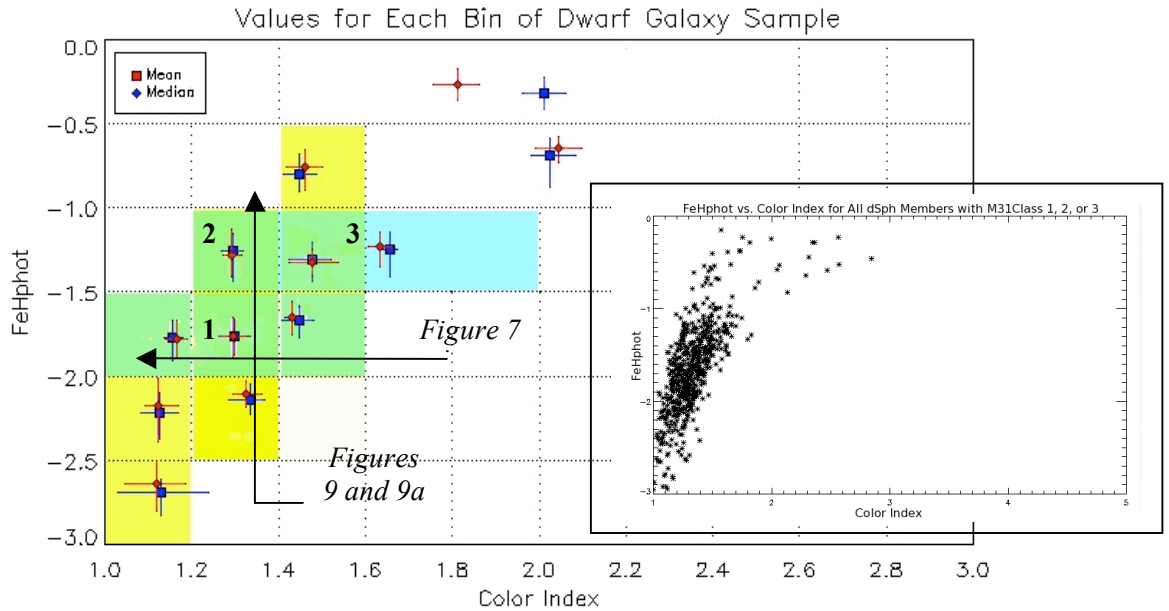
9

Figure 5: **The Mean and Median Values (with Root Mean Square Deviation) of Metallicity vs. Color for the Coadded Spectra of Each Bin of the dSph Field Sample**

In *Figures 4* and *5* (page 8, above), the highlighted portions signify rows of constant FeHphot (horizontal) or constant $(V-I)_0$ (vertical) usable for the ladder plots of coadded spectra. Ladder plots are extremely useful in viewing trends in the changing chemical makeup of the spectra as [Fe/H] is held constant while Color Index is increased (or vice versa). Note that the bins pictured in the figures are not the equal-sized bins first used to grid the Metallicity graphs, but rather are the "adjusted bins" generated to ensure that at least 10 star spectra were being coadded and that the coadded spectra are as accurate as possible. *Figures 4* and *5* are especially important, as they display the adjusted bins' shifted mean and median. Just based on the graphs above, the ideal locations for dSph and Field analyses and comparisons are visible.

III. Results and Discussion

By analyzing the calculated coadded spectra in various different ways, comparisons were made between and conclusions were drawn about the Field Sample and the dSph Sample.

A. Spectral Changes for Each Sample

Ladder plots were generated for each relevant row and column of the metallicity graphs generated in *Section II.D.* (See highlighted portions of *Figures 4* and 5). Rows and columns deemed 'relevant' included three or more bins (four for the Field Sample) and had spectra with well-centered mean and median FeHphot vs. $(V-I)_0$ values in individual bins. Ladder plots were the best way of seeing direct spectral changes with either changing Color Index or changing

Metallicity. Through analyzing the dramatic appearance, growth, or reduction of spectral

absorption lines, certain conclusions could be made about the Field Sample and the dSph Sample

1. Spectral Changes seen as a function of $(V-I)_0$ at a given FeHphot range

First, spectral changes seen as a function of $(V-I)_0$ at a given FeHphot range were

observed (rows for both the Field and dSph sample). For the former, three ideal rows were

selected, of which one is shown below (*Figure 6*). (Results for ideal rows and columns not
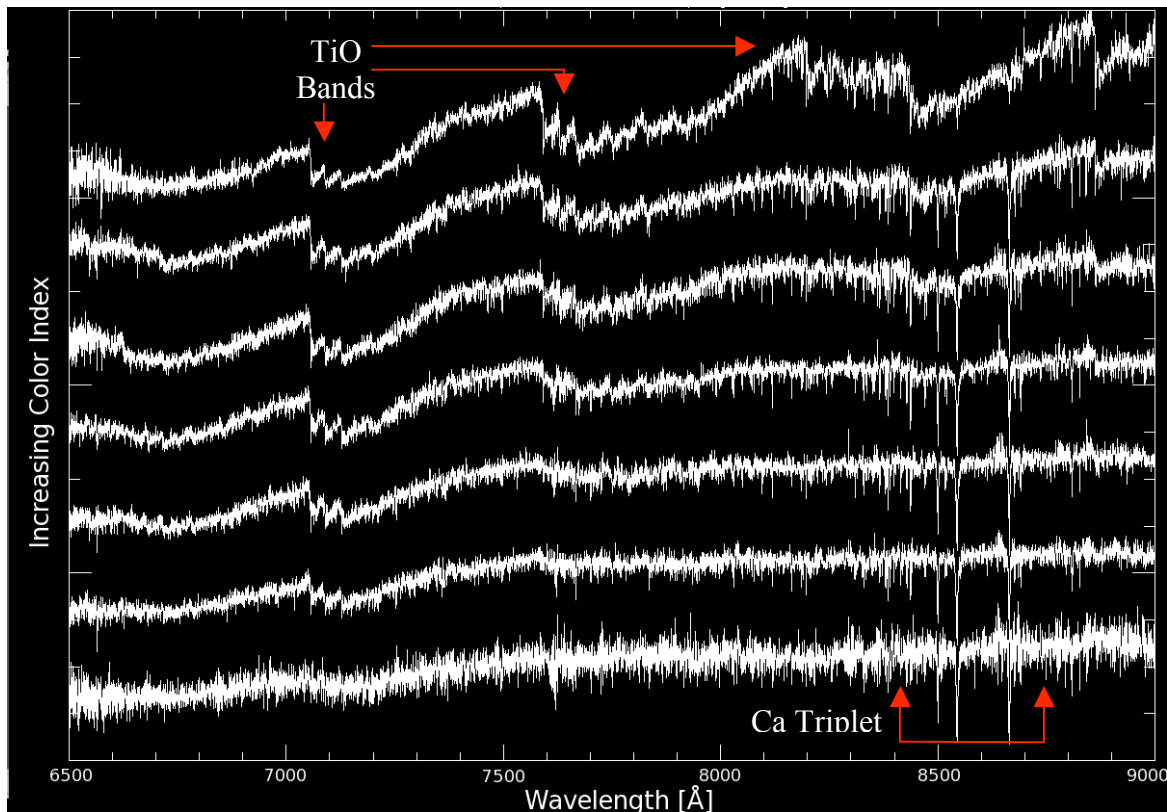
pictured were consistent with listed results).

Figure 6: **Spectra (Wavelength [Å]) of Field Stars with FeHphot= [-0.5, 0.0] and Increasing**

From simply looking at the whole spectra, distinct changes can be seen as $(V-I)_0$ increases. TiO bands
(noticeable by their jagged, step-like appearance) appear at 7100 [Å] for the top six spectra, are clearly
visible at 7600 [Å] for multiple spectra, and even appear at approximately 8200 [Å] for the spectrum with
the largest $(V-I)_0$. To see specific fluctuations, the Ca triplet (8498 [Å], 8542 [Å], and 8662 [Å]) was
observed (*Figure 6a*).

In addition, because this particular row has quite a few bins, a *quantitative* analysis of the

changes in absorption lines is possible, practical, and relevant (although not necessarily so in the

11

cases of the dSph spectra). By analyzing a portion of the spectra without absorption lines and

comparing it to a section with an absorption line, an IDL program calculated the equivalent

width of absorption lines, or rather, the

amount by which an absorption line varies

from the rest of the spectrum. In *Figure 6a*

below, the total equivalent widths of the Ca

triplet are graphed as a function of

increasing color. Judging from the graph on

the right, the change in strength of the Ca

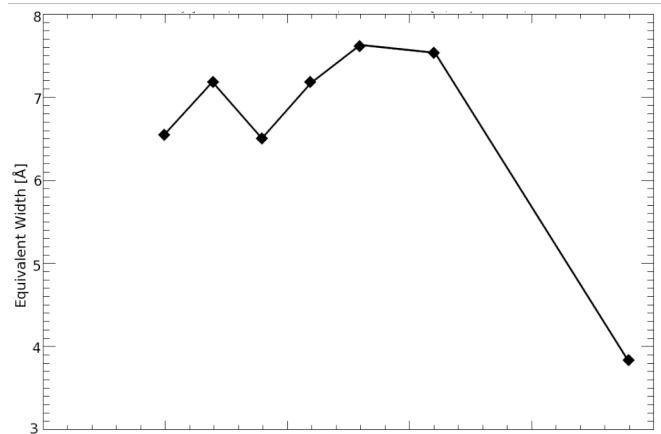triplet absorption lines is not monotonic:

Figure 6a: **Changing Total Equivalent Widths (0.1 [Å]) for Average of Ca Triplet Absorption Lines in Field Sample (with FeHphot=[-0.5, 0.0] and Increasing Vi0)**

when FeHphot is kept constant, certain star $(V-I)_0$ values have a higher level of metallicity, but

the strength of the lines do not increase proportionally to color.

For the dSph sample, two ideal rows were selected, of which one is displayed below

(*Figure 7*). The dSph sample also reflected a non-monotonic change in spectra, visible by

observing at 6600 [Å], 7600 [Å], and by inspecting the Ca Triplet's changes.
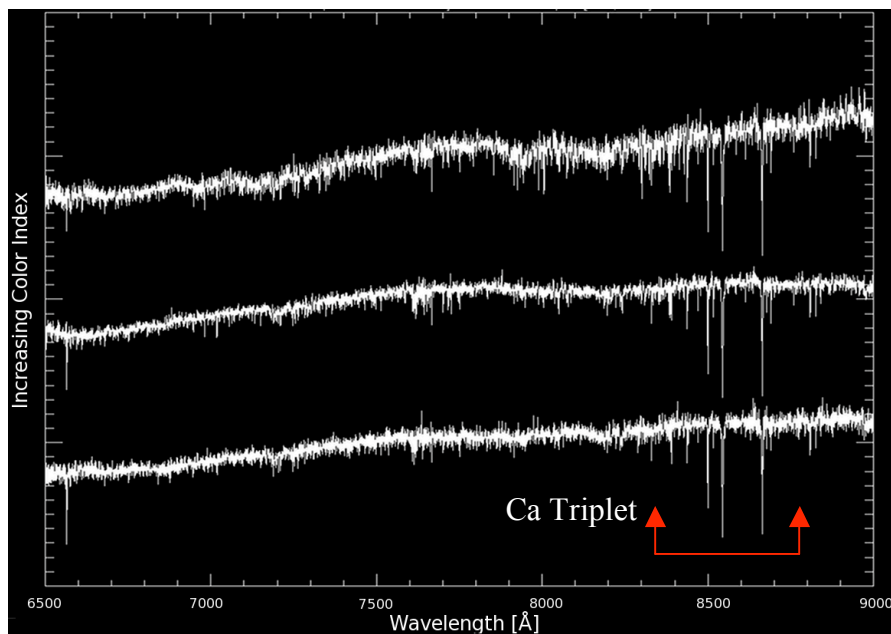

Figure 7: **Spectra (Wavelength [Å]) of dSph Stars with FeHphot= [-1.5, -1.0] and Increasing Vi0 (Color Index)**

2. Spectral Changes seen as a function of FeHphot at a given (V-I)$_0$.

Next, spectral changes seen as a function of FeHphot at a set (V-I)$_0$ range were observed (columns for both the Field and dSph sample). These observations were perhaps even more important than those outlined in *Section III.B.* because the chemical changes based on color could be accurately approximated (the appearance of TiO bands, for example), while the chemical changes based on Metallicity were relatively uncertain (Lagutin & Pchelina 2004). For the Field sample, three ideal columns were selected, of which one is displayed below (*Figure 8*).
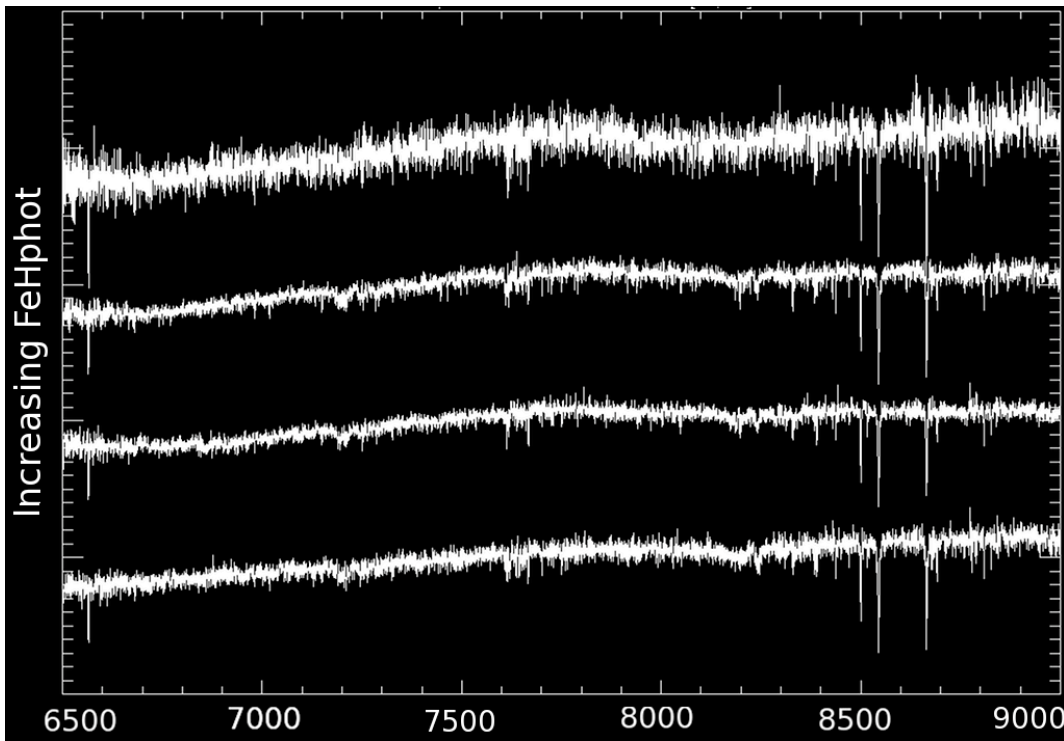

Figure 8: **Spectra (Wavelength [Å]) of Field Stars with Vi0=[1.2, 1.4] and Increasing FeHphot**

From this ladder plot, signs of chemical trends are clearly visible. Absorption lines seem to be getting sharper and deeper as FeHphot increases: in particular at 6500 [Å], 7600 [Å], and around the Ca triplet area. Closer inspection of this area reveals that each Ca line does become stronger with increasing FeHphot, and, in addition, weaker metal absorption lines in between the Ca lines become stronger at 8460, 8560, 8675, and 8690 [Å] (See *Figure 8a* below).
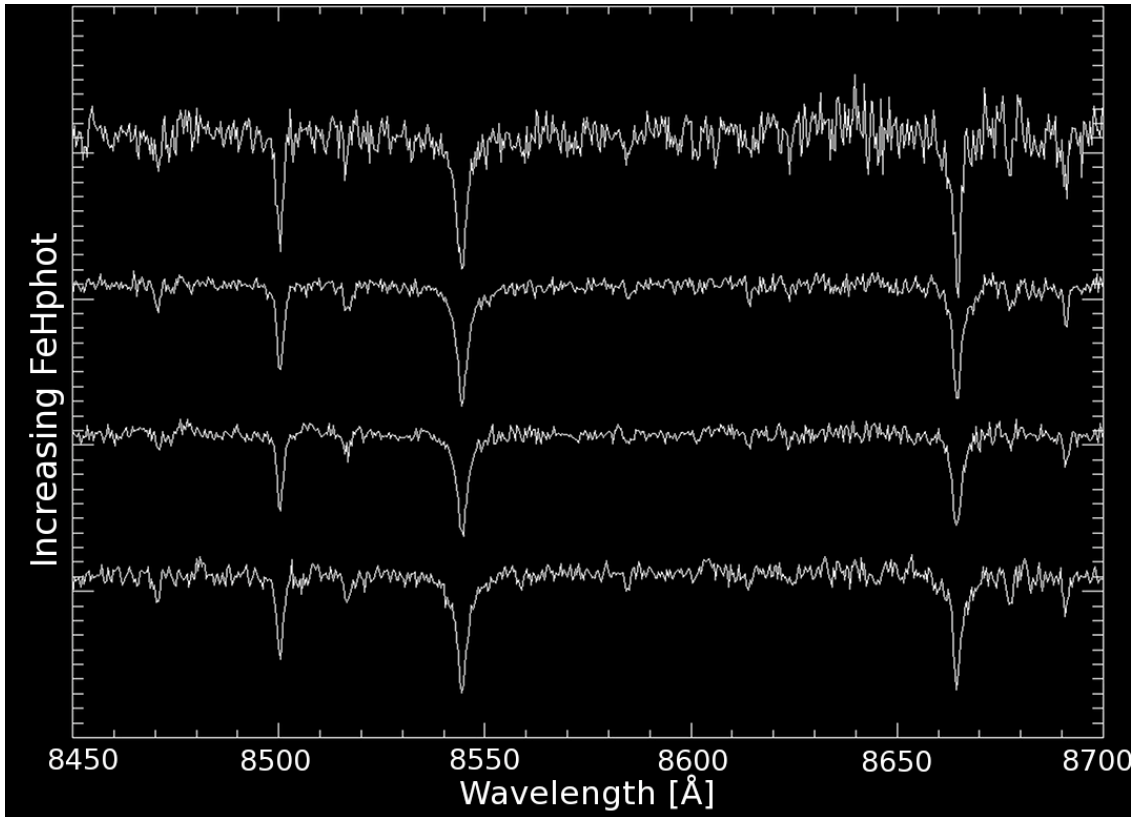
Figure 8a: **Ca Triplets of Spectra (Wavelength [Å]) of Field Stars with Vi0=[1.2, 1.4] and Increasing FeHphot**

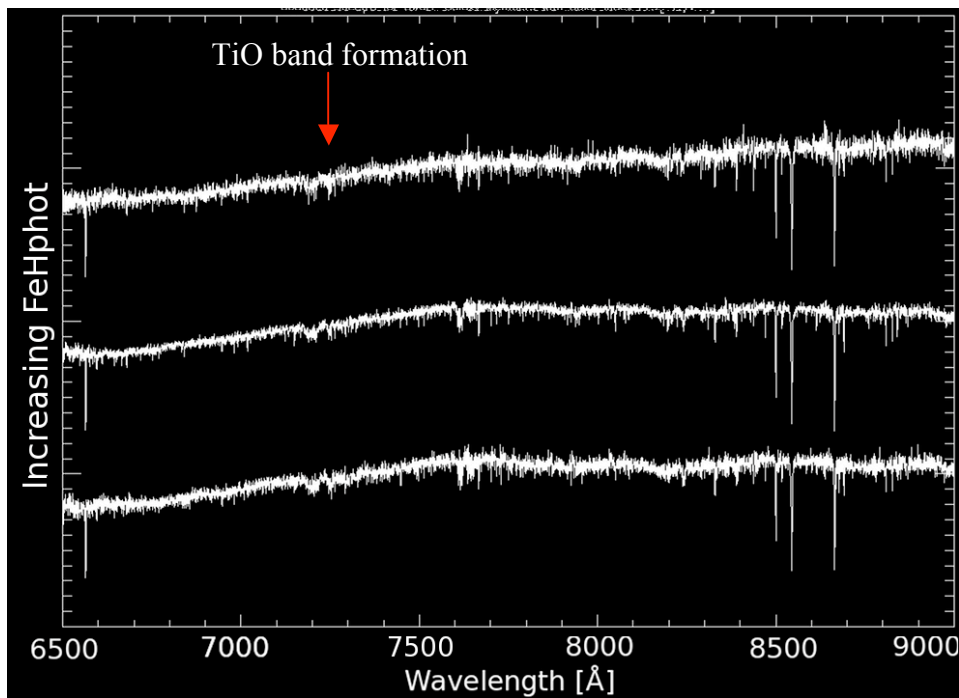For the dSph sample, two ideal columns were selected, one of which is displayed below:

Figure 9: **Spectra (Wavelength [Å]) of dSph Stars with Vi0=[1.2, 1.4] and Increasing FeHphot**
In addition to the chemical trends seen in the Field Sample, beginnings of TiO band formation are visible in this plot at around 7150 [Å]. The Ca band trends are visible in *Figure 9a*.
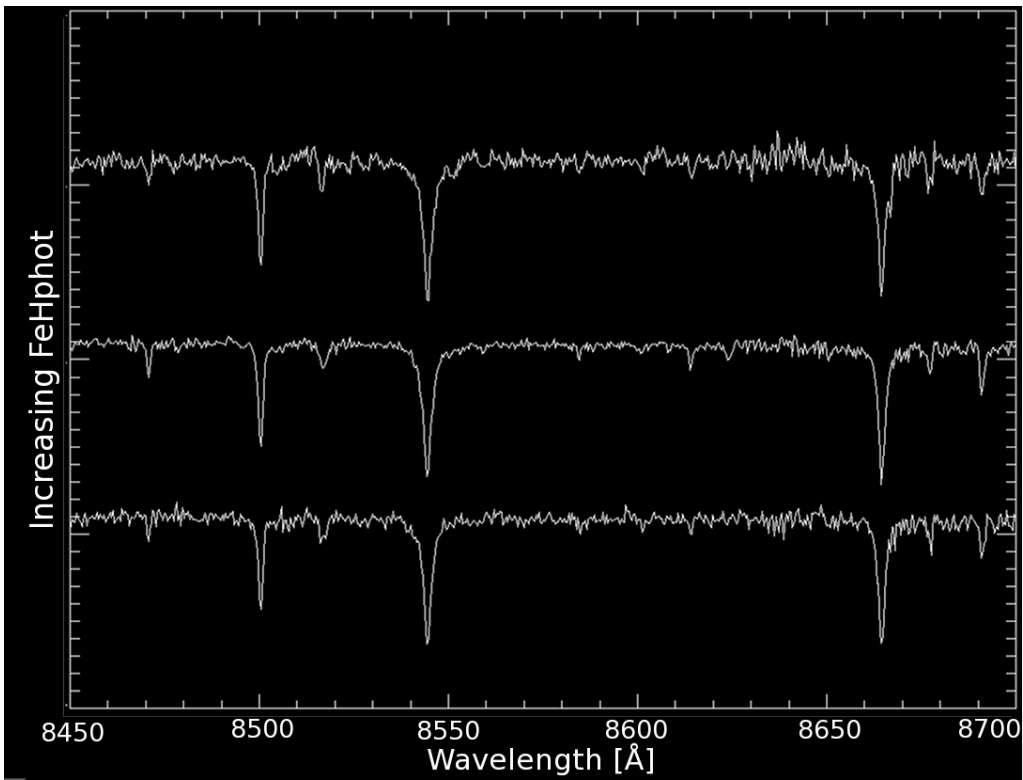
Figure 9a: **Ca Triplets of Spectra (Wavelength [Å]) of dSph Stars with Vi0=[1.2, 1.4] and Increasing FeHphot**

Figure 9a shows the increasing strength of the Ca Triplets as FeHphot increases. The spectral lines become deeper, sharper, and wider. The chemical trends seen from the Field Sample analysis are reinforced by the dSph Sample results (both *Figures 9* and *9a*). Absorption lines seem to be getting stronger (for most elements) with increasing FeHphot.

B. dSph vs. Field Comparison

First, dSph Members and Field Stars at a given FeHphot and $(V-I)_0$ (Single Bin) were compared. Bins with a large number of stars for both samples were the ideal locations for this comparison. As a result, the bins outlined in *Table 1* were selected for the Single Bin comparison (only Bin 2 is detailed in this paper, but the other two bins reflected the same results).

Table 1: **Bins selected for Single Bin dSph vs. Field Comparisons**

	$(V-I)_0$ [mag]	FeHphot [dex]	Number of Stars in dSph Sample	Number of Stars in Field Sample
Bin 1	[1.2, 1.4]	[-2.0, -1.5]	168	47
Bin 2	[1.2, 1.4]	[-1.5, -1.0]	84	88
Bin 3	[1.4, 1.6]	[-1.0, -0.5]	21	81

Bin 1has a larger number of dSph stars, Bin 2 is relatively even, and Bin 3 is skewed in favor of the Field Sample. However, all three bins have a large number of stars in both metallicity graphs, a requirement for this type of comparison. The bins are labeled on *Figures 4* and *5* for reference.
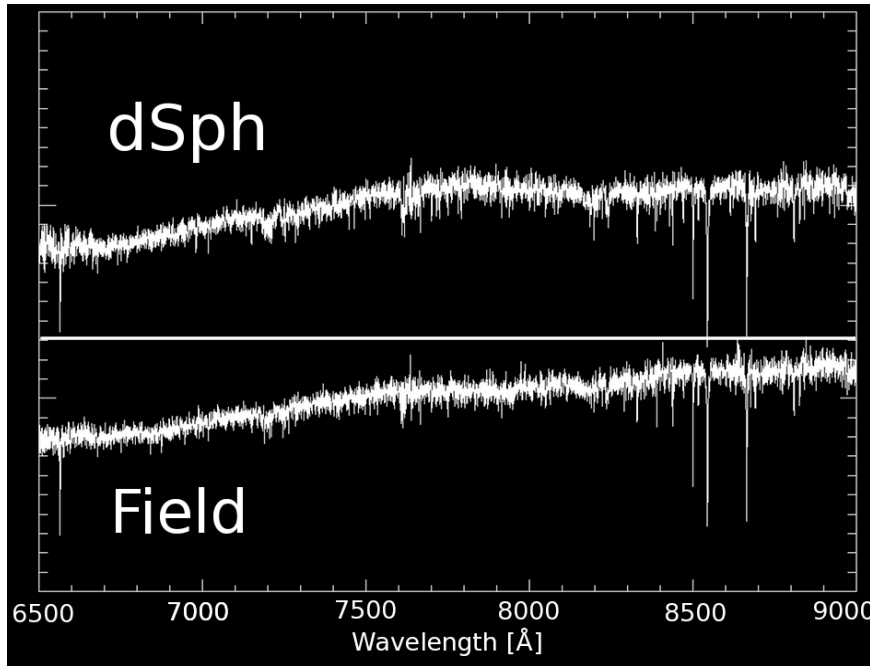
Just from immediate inspection of *Figure 17* (left), it is clear that at a given FeHphot (metallicity), both the field and the dSph populations have a very similar mix of stars. For the spectra to be so similar at a given Vi0 and FeHphot, the stars most likely have very similar [α/H] ratios. However, closer inspection is needed to draw conclusions about Fe or to determine whether the dSph and Field populations are chemically identical.

Figure 10: **Bin 2(Spectra (Wavelength [Å]) of Field and dSph Stars with FeHphot= [-1.5, -1.0] and Vi0= [1.2,1.4]**
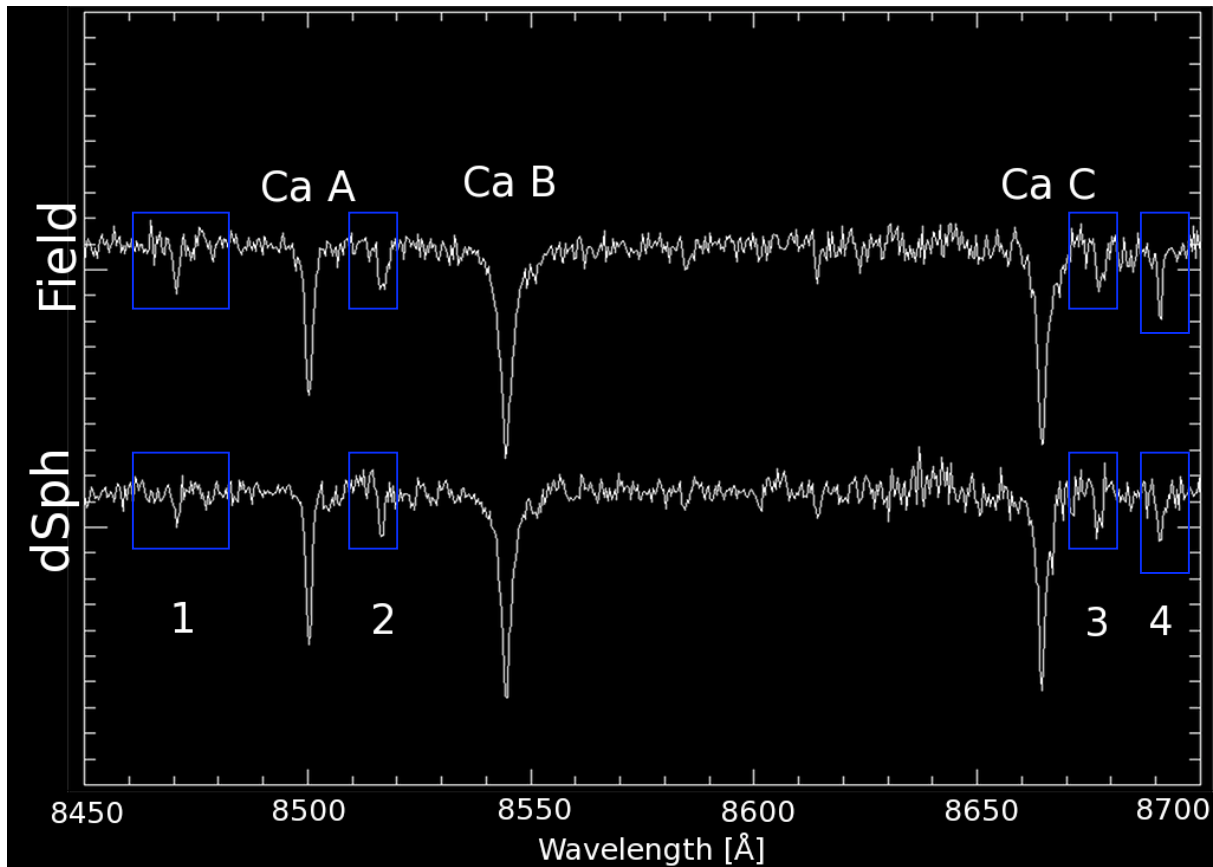

Figure 10a: **Ca triplets and Weaker Metal Absorption Lines for Bin 2 (Spectra (Wavelength [Å]) of Field and dSph Stars with FeHphot= [-1.5, -1.0] and Vi0= [1.2,1.4]**

Although both spectra are extremely similar, the Field spectra seems to have larger equivalent widths at each absorption point, as well as a larger "base" where the absorption line connects with the spectra.

Table 2: **Equivalent Widths for Ca Triplets and Weaker Metal Absorption Lines for Bin 2**

	Average Ca Triplet	1 (8468- 8472 [Å])	2 (8512- 8520 [Å])	3 (8660- 8670 [Å])	4 (8690- 8697 [Å])
dSph Equivalent Width	44.47 [Å]	10.96 [Å]	16.46 [Å]	19.87 [Å]	19.74 [Å]
Field Equivalent Width	54.51 [Å]	22.15 [Å]	20.34 [Å]	20.36 [Å]	20.25 [Å]

In *Table 2*, the Field Sample's equivalent widths are all greater than the dSph Sample's, even for the weaker metal absorption lines. Both quantitatively and qualitatively, it is clear that the Field Sample has stronger absorption lines and is more chemically enriched than the dSph Sample, although not by much. Thus, although the two populations have stars with similar substance, the Field Sample is chemically richer. Bins 1 and 3 also reflected this finding.

Next, dSph Members and Field Stars at a given FeHphot and increasing $(V-I)_0$ were compared to see the differences in chemical trends for the two samples. The best overlap for the dSph Sample and the Field Sample for a given FeHphot but increasing $(V-I)_0$ seemed to be when FeHphot = [-1.5, -1.0] In addition dSph Members and Field Stars at a given $(V-I)_0$ and increasing FeHphot were compared to see if there were other differences in chemical trends between the two populations. The best overlap for the dSph Sample and the Field Sample for a given $(V-I)_0$ but increasing FeHphot seemed to be when $(V-I)_0$ = [1.2, 1.6] (See *Figures 4* and *5*). However, these two comparisons revealed findings corroborated by the *Section III.A.* analyses: the chemical trends of these two populations are extremely similar, while the chemical composition of the two populations differ.

IV. Conclusions and Future Steps

A. The Coaddition Process: One key difference between this study and other chemical analysis projects was the use of coadded spectra. This process amplified any common chemical trends within a small "population" (bin), and in the process, properly analyzed data with low signal-to-

noise ratios. For both the dSph and Field population, trends as a function of FeHphot (with all else fixed) or as a function of $(V-I)_0$ *were seen*. These trends prove that the process of coaddition is fully capable of revealing trends in spectral features, amplifying what already exists so that a pattern can be located.

B. Chemical Analysis of the Field and dSph Samples: Overall, the study's results showed that changes in Metallicity and Color not only have an effect on a star's spectrum, but also change in consistent patterns. Similar spectra for the two samples led to the conclusion that both populations have a similar mix of stars; the difference, however, lies in the chemical enrichment of the populations. The spectral analysis conducted in *Section III* shows that the Field Sample is chemically richer. There are numerous reasons that could account for the discrepancy between the two samples. Perhaps the dSph galaxies are taking on some chemical properties of M31 itself (e.g. Majewski et. al 2007). It is also possible that the dSph galaxies have undergone transformations separate from M31. However, one idea remains certain: the origin of the dSph galaxies (as seen by its chemical composition) is distinctly different from that of M31 itself.

C. Future Steps

There are several possible steps that can be taken to further analyze the chemical enrichment history of M31 by focusing on its Field Stars and dSph stars. First, this project is groundbreaking in using coadded spectra, and, as a result, has the potential to help launch numerous studies on the entire galaxy that were previously impossible.

The next appropriate step includes extracting detailed abundances from the coadded spectra (e.g. Lee et. al 2008). Instead of simply analyzing changes in absorption lines or differences in various spectra, specific elemental information will be drawn from this study's spectra, information about elements such as Mg, Si, Ca, Ti (in this analysis, the metallicity

estimate used was only based on the [Fe/H] ratio) (e.g. Kirby et. al 2008). This project has already become the basis for a study on the detailed abundances of M31's stars.

Furthermore, in this study stars from multiple dSph satellites were grouped together into one population; by observing individual dSphs around Andromeda and comparing them with each other, more conclusions can be drawn not just about M31's chemical essence but also about dSphs in general.

In terms of quantitative analysis, the Metallicity Distribution Function (MDF) of the dSphs can be taken into account. MDFs help expose information about star formation within dwarf galaxies by comparing [Fe/H] information for a dSph with different sample curves. The best curve fit then reveals the star formation history of the galaxy (Kirby et. al 2009). Overall, there is huge potential for the work conducted in this study to be the starting point for numerous other projects, as it has substantiated the coaddition process, revealed information about the chemical enrichment history of Andromeda, and has highlighted subtle yet key differences between the Field population and dSph population of the Milky Way's sister galaxy.

References

Côté, P., Oke, J. B., Cohen, J. G., 1999, Astronomical Journal, 118, 1645-1656

Cox, T. J., Loeb, A., 2007, arXiv:07051170v2

Forgan, D., 2008, arXiv:astro-ph/08102222

Gilbert, K. M., Font, A. S., Johnston, K. V., Guhathakurta, P. 2009, Astrophysics Journal.

Gilbert, K. M., Fardal, M., Kalirai, J. S., Guhathakurta, P., Geha, M. C., Isler, J., Majewski, S. R., Ostheimer, J. C., Patterson, R. J., Reitzel, D. B., Kirby, E. N. 2007, ApJ. arXiv:astro-ph/09081111

Gilbert, K. M., Guhathakurta, P., Kalirai, J. S., Rich, R. M., Majewski, S. R., Ostheimer, J. C., Reitzel, D. B., Cenarro, A. J., Cooper, M. C., Luine, C., & Patterson, R. J. 2006, ApJ, arXiv:astro-ph/0605171v2

Guhathakurta et al., 2006, arXiv:astro-ph/0502366v5

Kalirai, J.S. et al. 2009, ApJ, arXiv:astro-ph/09093298

Kirby, E. N., Guhathakurta, P., Bolte, M., Sneden, C., & Geha, M. C. 2009, ApJ, in press, arXiv:astro-ph/09093092

Kirby, E. N., Guhathakurta, P., & Sneden, C. 2008, ApJ, 682, 1217

Lagutin, V. I., Pchelina, I.Z., 1985, Springer New York, 28, 49-51

Lee, Y. S., et al. 2008, Astronomy Journal, 136, 2022

Majewski, S.R. et. al, 2007, ApJ, arXiv:astro-ph/0702635v2

Morossi, C., Franchini, M., Di Marcantonio, P. & Malagnini, M. L. 2007, n.p., 3, 504-505

Smecker-Hane, T. & McWilliam, A. 1999, arXiv:astro-ph/9910211v1

Walker, M. G., Mateo, M., Olszewski, E. W., Gnedin, O. Y., Wang, X., Sen, B., & Woodroofe, M. 2007, ApJ, 667, L53

Yin, J., Hou, J. L., Prantzos, N., Boissier, S., Chang, R. X., Shen, S. Y., & Zhangh, B., 2009, arXiv:astro-ph/09064821